

Near-field photolithography with a solid immersion lens

L. P. Ghislain^{a)} and V. B. Elings

Digital Instruments, 112 Robin Hill Road, Santa Barbara, California 93117

K. B. Crozier, S. R. Manalis, S. C. Minne, K. Wilder, G. S. Kino, and C. F. Quate^{b)}

E. L. Ginzton Laboratory, Stanford University, California 94305-4085

(Received 9 September 1998; accepted for publication 20 November 1998)

We have exposed 190 nm lines in photoresist by focusing a laser beam ($\lambda=442$ nm) in a solid immersion lens (SIL) that is mounted on a flexible cantilever and scanned by a modified commercial atomic force microscope. The scan rate was 1 cm/s, which is several orders of magnitude faster than typical reports of near-field lithography using tapered optical fibers. The enhanced speed is a result of the high optical efficiency (about 10^{-1}) of the SIL. Once exposed with the SIL, the photoresist was developed and the pattern was transferred to the silicon substrate by plasma etching. © 1999 American Institute of Physics. [S0003-6951(99)05204-3]

The aggressive pursuit of ever decreasing features sizes on silicon integrated circuits has been a hallmark of the microelectronics industry. It is widely accepted that features sizes below $0.10 \mu\text{m}$ are not feasible with optical projection lithography,¹ the dominant technique in manufacturing today. In the past, continuous improvements in resolution have been achieved by decreasing the illumination wavelength. However, this will be difficult to continue due to the lack of suitable materials for making lenses below $\lambda \sim 193$ nm. Nevertheless, economic and device performance-related incentives exist for continuing to decrease feature sizes below $0.10 \mu\text{m}$ and a number of potential successor techniques are being researched; these include x-ray lithography, extreme ultraviolet (EUV) lithography, electron beam lithography, and scanning probe lithography.

Scanning probe lithography is promising because of its excellent resolution² (e.g., 20 nm) and because it does not require masks. However, like an electron beam system, the use of a single scanning probe for lithography is not economically viable for integrated circuit manufacturing because each pixel is exposed in a sequential fashion, making the lithography process unprofitably slow. However the progress that has been made recently in manufacturing high resonant frequency probes in parallel arrays^{3,4} has resulted in substantial improvements in throughput. Dense arrays of scanning probes could meet the requirements for resolution, throughput, and overlay.

We report near-field lithography using a solid immersion lens (SIL) mounted on a cantilever and scanned while in contact with the resist-coated sample. Fast scanning speeds are possible because the transmission efficiency of the SIL is about 10^{-1} . Dense parallel arrays of these devices will be realizable if a method to miniaturize them is found.

Near-field lithography uses a near-field scanning optical microscope (NSOM)⁵ to deliver light to a photosensitive sample. In the past, tapered optical fibers⁶⁻¹¹ and micropipettes¹² have been used for near-field lithography, but they are not practical for use in integrated circuit manufacturing due to slow scanning speeds (e.g., $80 \mu\text{m/s}$).⁸ Tapered fibers do not propagate waves in the region where the

diameter of the fiber is less than $\sim \lambda/2n$. In these regions the waveguide is in cutoff and the losses are exponential with distance. The exponential attenuation over the long taper of the fiber leads to typical transmission efficiencies of 10^{-4} to 10^{-7} ,^{10,11} which necessitates the use of slow scanning speeds. In addition, it would be difficult to integrate tapered optical fibers into dense parallel arrays.

The solid immersion lens operates on the same principle as the liquid immersion microscope, improving the resolution by increasing the refractive index of the gap between the lens and sample.^{13,14} The SIL microscope replaces the liquid with a high refractive index solid ($n_{\text{SIL}} \sim 2.2$). Since there is no aperture or pinhole, the classical Abbe diffraction limit $d \approx \lambda/2NA$ determines the resolution, where the numerical aperture $NA = n_{\text{SIL}} \sin \Theta$, and Θ is the half-angle of the cone of illumination. Due to total internal reflection for rays incident above the critical angle, the SIL can improve resolution only when the sample gap is less than about 50 nm. We recently reported a laser-scanning solid immersion microscope¹⁵ using a super-hemispherical SIL polished to produce a cone with a sharp tip ($\sim 1 \mu\text{m}$ radius). In this system, a laser beam focuses to a diffraction limited spot, ~ 150 nm full-width at half-maximum (FWHM) within the tip-sample contact area. In addition, we mount the SIL on a cantilever and use optical lever force feedback to control the tip-sample forces and keep the sample within the near-field of the SIL illumination (Fig. 1). Thus, the laser-scanning solid immersion micro-

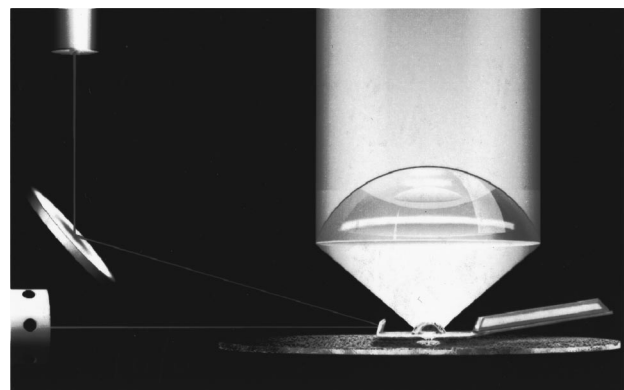


FIG. 1. Schematic diagram of the near-field scanning solid immersion microscope with the SIL probe mounted to a cantilever in an AFM.

^{a)}Electronic mail: luke@di.com

^{b)}Electronic mail: quate@stanford.edu

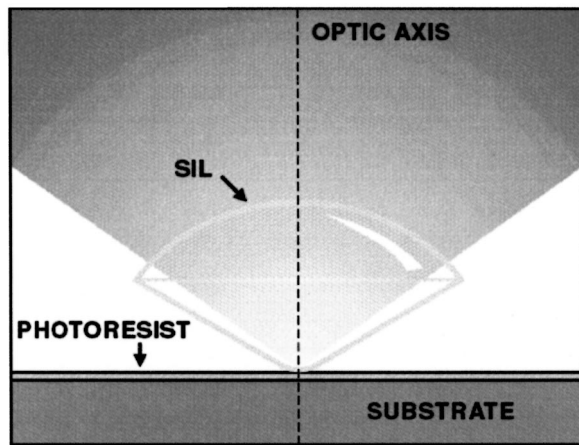


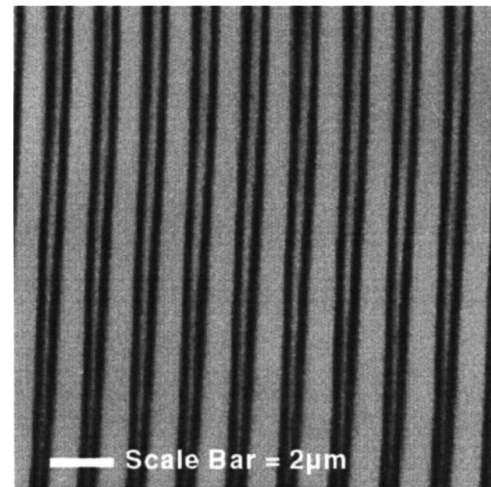
FIG. 2. Schematic diagram showing the SIL probe in position to expose photoresist.

scope provides a height image simultaneous with optical contrast. This capability would enable accurate overlay to be carried out in lithography.

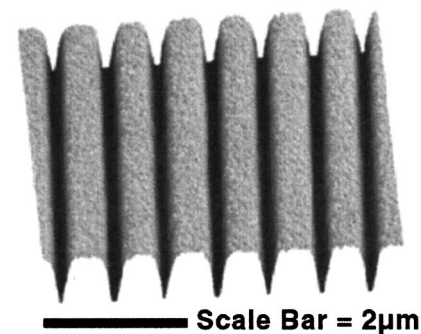
The schematic in Fig. 1 shows the cantilevered SIL probe combined with the optical lever sensor. This cantilever deflection sensor accommodates a high numerical aperture microscope objective ($100\times$ magnification, 0.73 NA) by sending a laser beam in from the side. The metal-foil cantilever carrying the SIL has a bend near the end that forms a reflector. A red laser diode beam focuses on the reflector and the returning beam bounces off a steering mirror onto a position-sensing detector. The detection method, called side-fire atomic force microscope (AFM), provides force feedback with a deflection sensitivity comparable to conventional AFM and can operate simultaneously with the exposure of photoresist.

To demonstrate photolithography, we have used the near-field illumination of the SIL to expose a 50 nm layer of photoresist (Shipley SPR 3001) spun on a silicon wafer (Fig. 2). A blue laser beam from a helium:cadmium laser at 442 nm enters the microscope objective and converges to a spot at the SIL tip. The photoresist was exposed as the piezotube scanner (not shown) scanned the sample in a raster pattern at about 1 cm/s ($100\ \mu\text{m}$ scan size, 50 Hz scan rate). If we increase the scan rate, we also increase the blue laser optical power to maintain the photon dose. The side-fire AFM allows the hemispherical SIL to contact and track the surface at high scan rates. In addition, we stabilize the SIL at high scan rates by increasing the stiffness of the metal-foil cantilever. We found no evidence of SIL tip or photoresist damage. The maximum speed of the SIL was limited only by the mechanical resonance frequency of the piezotube scanner.

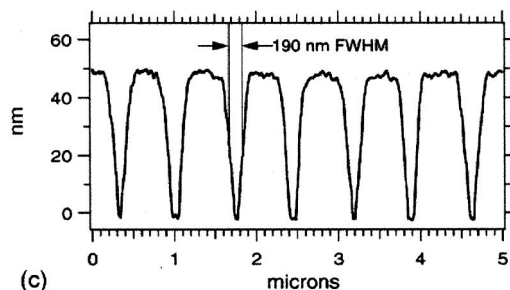
After exposure, we developed the pattern for 5 s in Shipley MF-319 and used an AFM operating in tapping mode to measure the linewidth. Figure 3(a) is a $15\ \mu\text{m}$ AFM scan of a pattern exposed at about 1 cm/s. The bottom of Fig. 3(a) shows the lines converging as the SIL approaches the turnaround. There are 64 lines/frame, corresponding to a line pitch of about 800 nm in the center of the frame. Figure 3(b) is a surface plot of a $5\ \mu\text{m}\times 5\ \mu\text{m}$ AFM scan showing evenly spaced lines with a pitch of about 700 nm near the center of the raster pattern. The typical line width is 190 nm FWHM and the depth is about 49 nm, as shown in Fig. 3(c).



(a)



(b)



(c)

FIG. 3. (a) AFM scan of lines in photoresist exposed with the SIL at a scan rate of $\sim 1\ \text{cm/s}$ ($15\ \mu\text{m}\times 15\ \mu\text{m}$ scan size). (b) $5\ \mu\text{m}\times 5\ \mu\text{m}$ AFM surface plot. (c) Cross-section of the lines in photoresist showing $\sim 190\ \text{nm}$ FWHM and $\sim 50\ \text{nm}$ depth.

To achieve a narrow linewidth we found that it is necessary to carefully optimize focus before exposure and, in some cases, sweep the focus over a small range during exposure. Since the SIL contacts the photoresist surface, the microscope objective determines the depth of focus, and the tolerance is $D_z \sim 0.9\lambda/\text{NA}^2 \sim 0.3\ \mu\text{m}$. Polarization also affects linewidth, so we orient the polarization along the x axis (the fast scan axis of the raster pattern) using a $\lambda/4$ - and $\lambda/2$ waveplate.

The developed resist patterns were transferred into the silicon substrate through etching in a LAM Research Systems TCP9400 reactive ion etcher. Prior to etching, the wafers were baked at $110\ ^\circ\text{C}$ for 30 min. The high density plasma generated using $\text{HBr} + \text{O}_2$ gases results in anisotropic etch profiles. The patterns were etched $\sim 0.3\ \mu\text{m}$ into the silicon. The resultant patterns (Fig. 4) were imaged using an

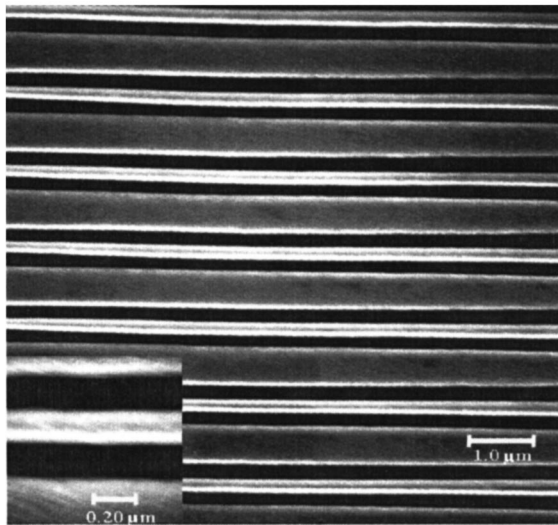


FIG. 4. SEM micrograph of sample after etching. Lines have been exposed by SIL in photoresist and then transferred into silicon by plasma etching. Etch depth is approximately $0.3 \mu\text{m}$.

Hitachi S-800 scanning electron microscope (SEM) operating at 25 keV. From the inset of Fig. 4, the lines are measured to be $0.23 \pm 0.01 \mu\text{m}$ (FWHM) and the space between the lines is $0.18 \pm 0.01 \mu\text{m}$ (FWHM).

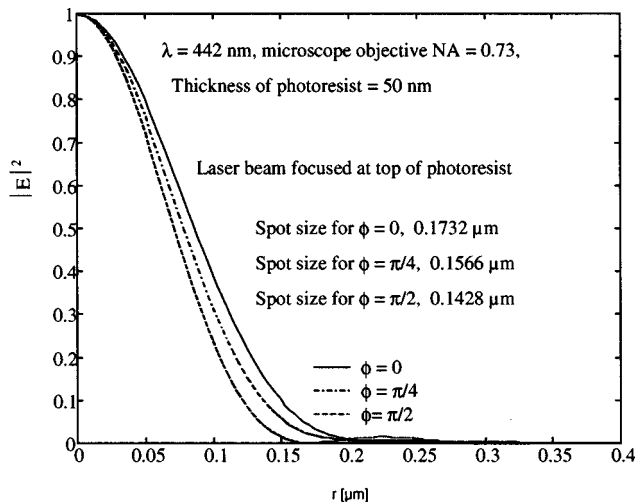


FIG. 5. Theoretical prediction of $|E^2|$ PSF for SIL in contact with photoresist film.

The point spread function (PSF) for the SIL operating in contact with the photoresist film has been theoretically calculated and is shown as Fig. 5. This calculation is based on Richard and Wolf's vector optic theory.¹⁶ The square of the electric field (E^2) rather than the power intensity has been calculated. In lithography the resolution is determined by the power absorbed in the photoresist, which is given by $\sigma \cdot E^2$ where σ is the conductivity of the photoresist. It is observed from Fig. 5 that the E^2 PSF is sensitive to polarization, meaning that the beam spot is elliptical in shape. The FWHM is $0.14 \mu\text{m}$ for $\phi = \pi/2$ polarization, but $0.17 \mu\text{m}$ for $\phi = 0$ polarization.

Near-field photolithography has been carried out with a scanning solid immersion lens with force control. A 190 nm linewidth in photoresist was achieved at a scan rate of 1 cm/s. This is considerably faster than the speeds that have been demonstrated with tapered optical fibers due to the superior transmission efficiency of the SIL. Future work will involve miniaturizing the SILs so that they may be fabricated in dense parallel arrays.

- ¹National Technology Roadmap for Semiconductors (Semiconductor Industry Association, San Jose, 1997).
- ²E. S. Snow and P. M. Campbell, *Appl. Phys. Lett.* **64**, 1932 (1994).
- ³S. C. Minne, J. D. Adams, G. Yaralioglu, S. R. Manalis, A. Atalar, and C. F. Quate, *Appl. Phys. Lett.* **73**, 1742 (1998).
- ⁴S. C. Minne, G. Yaralioglu, S. R. Manalis, J. D. Adams, J. Zesch, A. Atalar, and C. F. Quate, *Appl. Phys. Lett.* **72**, 2340 (1998).
- ⁵D. W. Pohl, W. Denk, and M. Lanz, *Appl. Phys. Lett.* **44**, 651 (1984).
- ⁶S. Wegscheider, A. Kirsch, J. Mlynek, and G. Krausch, *Thin Solid Films* **264**, 264 (1995).
- ⁷I. I. Smolyaninov, D. L. Mazzoni, and C. C. Davis, *Appl. Phys. Lett.* **67**, 3859 (1995).
- ⁸S. Madsen, M. Mullenhorn, K. Birkelund, and F. Grey, *Appl. Phys. Lett.* **69**, 544 (1996).
- ⁹E. Betzig and J. K. Trautman, *Science* **257**, 189 (1992).
- ¹⁰G. A. Valaskovic, M. Holton, and G. H. Morrison, *Appl. Opt.* **34**, 1215 (1995).
- ¹¹G. Tarrach, M. A. Bopp, D. Ziesel, and A. J. Meixner, *Rev. Sci. Instrum.* **66**, 3569 (1995).
- ¹²M. Rudman, A. Lewis, A. Mallul, V. Haviv, I. Turovets, A. Shchemelinin, and I. Nebenzahl, *J. Appl. Phys.* **72**, 4379 (1992).
- ¹³S. M. Mansfield and G. S. Kino, *Appl. Phys. Lett.* **57**, 2615 (1990).
- ¹⁴S. M. Mansfield, W. R. Studemund, G. S. Kino, and K. Osato, *Opt. Lett.* **18**, 305 (1993).
- ¹⁵L. P. Ghislain and V. B. Elings, *Appl. Phys. Lett.* **72**, 2779 (1998).
- ¹⁶B. Richards and E. Wolf, *Proc. R. Soc. London, Ser. A* **253**, 358 (1959).